NEW DEVELOPMENTS IN ROTOR WAKE METHODOLOGY

K.D. Brown[1] and S.P. Fiddes[2],
Department of Aerospace Engineering, University of Bristol
Bristol, UK

Abstract

A robust approach to rotor free wake calculations is described. The present method differs from earlier approaches in several aspects. The first is the dynamic merging of vortices. In many previous methods the amount and location of the merging of vortices is prescribed before the relaxation process has begun. The second difference is in the detailed and efficient treatment of the far wake influence for both accurate calculations of velocity and potential. Finally a relaxation scheme new to rotor modelling has been investigated and compared to other relaxation algorithms. The dynamic vortex merging approach was found to provide a robust and generalised approach to rotor wake modelling. The relaxation method was able to give converged results for hovering rotor cases for a full-span wake. While another relaxation algorithm was found to be quicker for a simple test case, it was unable to achieve full-span wake convergence in hover with its current state of development.

The developed free wake method has been coupled to both lifting-line and panel method representations of the blade. Good comparisons with experiment have been achieved for both hovering rotor and wind turbine configurations.

Notation

Symbols

c_θ axial distance between two vortices at start of far wake.

D $\sqrt{r_i^2 + r_v^2 + X^2}$

h_s height of conical section

m_θ difference in pitch between outer and inner bounding vortices (of a helical strip)

$\hat{n}$ unit normal to doublet surface

N number of blades

p wake pitch $(dx/(Rd\theta))$

$\mathbf{q}$ vector $[q_x, q_y, q_z]$ from a point on a doublet surface to a velocity potential evaluation point

q $|\mathbf{q}|$

r radius divided by the tip radius

R rotor tip radius

S area

x axial coordinate divided by the tip radius

X $-q_x$

θ azimuth angle (angle of rotor rotation)

μ doublet strength

ϕ velocity potential

Subscripts

b base of conical section

i potential/velocity evaluation point

m midway along a helical strip at the azimuth angle where the far wake commences

t top of conical section

v point on the wake/doublet surface

Introduction

Full free-wake calculations have been shown to be essential for accurate rotor performance predictions for cases where the wake is not quickly swept downstream, that is when the induced velocities become significant in comparison with the onset flow. The extreme case is that of a rotor without an onset flow such as a hovering rotor. Free wake calculations were first attempted for this extreme by Clark and Leiper [7]. This hovering rotor case has since received much attention with numerous approaches being devised. A common problem experienced with these methods is that of convergence. With basic relaxation algorithms, this problem can be circumvented by merging groups of discrete vortices together. This is usually done a short distance from the trailing edge of the rotor blade model, resulting in a strong tip vortex and a few inboard vortices. In

1990, Quackenbush et. al. [24] presented an alternative solution to the convergence problem. By using a semi-implicit algorithm they were able to obtain converged solutions for a hovering rotor. They also showed that while the solutions were self-preserving, they were unstable, which was why an implicit approach was required to obtain them. This method did have the unfortunate drawback of a computationally expensive numerical implementation; requiring a large (depending on the number of wake points) matrix inversion for each step of the calculation procedure. The instability came about in the form of vortices orbiting one another, as shown by a simple two-dimensional demonstration in their report. This phenomenon has indeed been observed in experiments. Landgrebe [17] reported this occurence during a wake visualisation study. This was, however, found to occur only after the wake had aged beyond two turns of the rotor. This would have little influence on the aerodynamic performance of the blades. Numerically, this phenomenon is far more widespread. This is mainly due to the continuous distribution of vorticity in the wake being modelled by discrete vortex filaments. The numerical merging of vortices in the wake can thus be thought of as the migration of vorticity across the width of the wake. Vortex merging is discussed in detail by Hopfinger and van Heijst [12], where merging criteria based on empirical observations are reviewed. The relevance of empirical vortex merging to the free wake numerical algorithm depends on whether the sheet of vorticity shed from the trailing edge of a rotor blade, rolls up into discrete vortices. This is not generally the case. The main effect of merging in a numerical scheme is therefore to stop the discrete vortices from orbiting one another. The amount of merging required to prevent arbitrarily orbiting vortices is one of the issues considered in this paper. Another common cause of convergence problems is the root vortex. For a hovering rotor, this has the lowest pitch of all the vortex filaments. In numerical methods, this can tend to move the root vortex over the following blade. Although this vortex is weak, it can present problems for the calculation of the blade loading as it moves towards the blade. Miller [19] encountered this problem while using his fast free wake method, and eventually assigned zero strength to the root vortex. With the dynamic approach to vortex merging and careful attention to the relaxation algorithm, the root vortex stayed below the following blade while reaching a converged solution for most of the hovering test cases encountered with the present method.

Vortex Merging Algorithm

The principal aim of merging the vortices is to stabilize the calculation by preventing vortices from continuously orbiting one another. A means must therefore be established to detect the occurence of orbiting vortex filaments. This problem was first considered by Moore [21] for an unsteady two-dimensional problem. In this approach, when three adjacent point vortices formed an angle less than $90°$, then the two with the smallest gap between them were merged together. This technique was later applied in three dimensions by Gaydon [10] for wakes shed from steady lifting surfaces. Moore's criterion was applied at each 'cross-flow' plane down the wake. The present algorithm is similar to that of Gaydon's but with a few important modifications required for rotor wakes. Modifications include the "logical" merging of the vortices and refinement of the merging criterion.

The merging of vortices in three dimensions actually creates a force in the wake. Consider the situation in the following figure.

local velocity vector
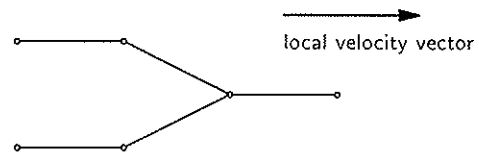
Figure 1: Merging of Two Discrete Vortices

It is impossible for two segments joining together to both be aligned with the local velocity. Therefore, there must exist a component of velocity normal to the vortex segments and hence a force. To minimize this force, the point at which the two vortex segments join, is calculated as a circulation weighted mean of the segment ends that would result if the two segments were aligned with their respective local velocity vectors. It is also worth noting that the length of the merging segments does not effect the force exerted on the wake since the component of the segment normal to the local velocity will remain the same.

As merging occurs, it is possible to significantly reduce the time required for wake influence calculations, since a merged group of vortices can be treated as a single vortex.

As in the method of Gaydon [10], there are two criteria for determining when to merge vortices together. These are the angle formed at a 'cross-cut' of the wake and the minimum distance apart, beyond which merging does not occur. Both the criteria are applied,

since if the vortices are too far apart then they won't be orbiting one another, and if they are too weak but close together, then they will also have little effect on each other. Both the effect of the angle and the minimum distance were investigated. The combination of the two which caused the least merging but resulted in converged wake solution is an angle specified in terms of its cosine as 0.13 and a minimum distance of $0.07R$, where R is the radius of the rotor. In addition, no merges are allowed to commence on the final row of free-wake vortex segments. The reason for this is due to the subsequent effect of the distorted orientation of these segments on the far wake (the pitch of which will be made equal to that of such segments).

In hovering rotor applications, the two criteria affect different parts of the wake. Within the inboard region of the wake, the vortices stay fairly close together, so it is changes to the angle criterion which has the most significant effect. Conversely, for the outer region of the wake (including the tip vortex and the outer part of the inboard 'sheet') it is the distance criterion which has the biggest impact. The angle criterion is usually met when considering the tip vortex along with the two outer vortices of the 'sheet'. The distance criterion thus has the most influence on the outer vortices of the inboard 'sheet'. These do have a tendency to orbit one another in cases where there is a significant increase in loading of the blade towards the tip. The existence of vortices of significant strength in this region have been observed in experiment [16].

Wake Influence Calculations

The wake is split into two regions; the fully relaxed near wake and the constant pitch and radius far wake. Each filament of the far wake is of the same pitch and radius of the last segment of the relaxed near wake. Each wake filament in the near wake is discretized into a series of straight line vortex segments. The influence of the near wake is therefore simply calculated using the Biot-Savart law. Although more efficient representations of vortex filaments exist [3, 4], the use of vortex line filaments provides a simple base on which to develop and investigate the present method. Further, the contribution to the velocity potential of wakes represented by the more advanced models has not been investigated.

The far wake is extended an infinite distance downstream. To make the calculation of the influence of the far wake efficient, the analytical approximation of

Wood and Meyer [27] was utilised. Gould [11] performed a survey of the various analytical expressions for the semi-infinite helical vortex and showed that the method of Wood and Meyer [27] was the most computationally efficient by a significant margin. Like the other analytical approximations, it is only accurate for velocity calculations beyond a given distance upstream of the start of the helix. A detailed study of the effect of the number of terms used in the analytical approximation and the helix pitch was presented by Brown and Fiddes [5]. For the analytical approximation of all three Cartesian velocity components to be accurate to within half a percent, the semi-infinite helix is required to be a distance downstream of the velocity evaluation point of;

$$\frac{\text{length of near wake}}{R} = 0.62\log\left(\frac{1}{p}\right) + 0.44. \quad (1)$$

The term p refers to the pitch of the vortex filament, which the axial distance travelled by the filament per radian of rotation. For the influence of a single isolated vortex, the above expression will not, in general, produce the specified accuracy. However, when the velocity influence of two trailers of a single horseshoe are summed together, their individual oscillations tend to cancel one another (since their strengths are of opposing sign). For any given point of required velocity evaluation, the above expression implies that, in general, there is a portion of the helix whose influence is not calculated. This occurs when the required distance is greater than that to the end of the near wake region. The influence of this 'intermediate' region is calculated by discretizing this part of the helix in the same manner as the near wake. The length of this intermediate portion of the wake will vary depending upon the point at which a velocity calculation is required and of course on the pitch of each vortex whose influence is being calculated. This ensures the most efficient calculation of the wake beyond that which is relaxed.

Furthermore, decreases in solution time were realised by the inclusion of an approximation to the Biot-Savart law calculation for cases where the line segment was many multiples of the segment length away from the velocity evaluation point. The approximation is the expression for a vortex particle.

For the panel method adopted here, the velocity potential influence of the wake is required. For the near wake, the influence of each doublet panel (using the equivalence with vortex rings) is calculated using the usual exact/approximate expressions that

are conventionally used for a hyperboloidal quadrilateral constant strength doublet panel [22, 23]. More so than for the velocity influence calculation, panels would have to be extended for a large distance downstream in order for there to be no change in velocity potential induced by the wake with respect to the extension of the wake downstream. An expression was thus developed to calculate the influence of a semi-infinite helical doublet strip bound by two helices (the vortices) of arbitrary differing pitches. This is a subject which has been largely ignored in the literature on the application of potential based panel methods to rotor prediction. Gould [11] developed an expression for the potential influence of a semi-infinite helix, but was limited to doublet strips bounded by helices of identical pitches starting at identical axial locations. That is, the pitch was not allowed to vary across the helical panel. This is inadequate for free wake calculations where the pitch does, in general, vary across the wake.

An expression which evaluates the far wake potential influence of the wake will now be presented. The expression for the potential ϕ which is required to be evaluated is

$$\phi = \sum_{n=1}^{N} \int \int \frac{\mu}{4\pi} \nabla \left(\frac{1}{q} \right) \cdot \hat{n} \, dS \qquad (2)$$

The summation is performed over the helices from the N blades of the rotor. The unit normal to the doublet surface is denoted by $\hat{n}$. The doublet strength is denoted by μ. The vector $\mathbf{q}$ extends to the velocity potential evaluation point from a point on the helical surface. The integral be evaluated over the surface S which exists between two trailing vortices, extending from a finite distance downstream to an infinite distance downstream. The form of the doublet surface is taken to be constructed from straight lines connecting the two trailing vortices at identical values of azimuth angle. The approach used to evaluate the integral is to consider the summation of the velocity potential influence of infinitesimal azimuthal segments of the helical strip. The influence of each strip is calculated using two approximations from the outset. The variation of the distance from points across an incremental strip to any given collocation point is neglected. This is a reasonable assumption since this is to be an expression valid for the far wake. Secondly, the unit normal to the strip at a given azimuth angle is taken to be an average value for the strip at that azimuth angle. The variation in pitch (the point of the current work) is taken into account in the calculation of the vertical

distance between the two bounding helices at any given azimuth angle. This will effect both the averaged unit normal and the incremental surface area.

The first step is to obtain an expression for an incremental surface area dS of the helix over an increment in azimuth angle $d\theta$. The area under a curve can be represented by a series of rectangles of diminishing width. Therefore, it is proposed that the area between two helices of differing pitch and radius can be formed by a series of conical sections of diminishing angle $d\theta$. This approximation is illustrated in figure 2.
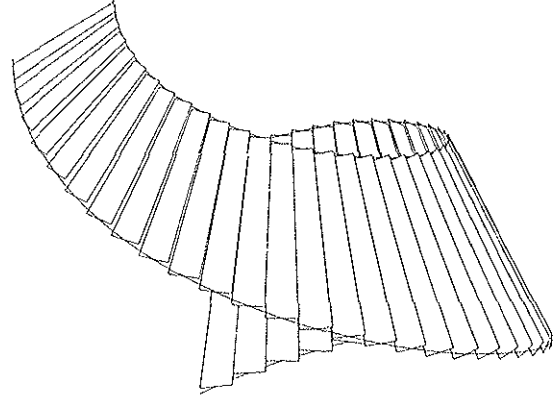
Figure 2: Helical Strip with Conical Section Increments

The area of a section of a conical frustrum can be derived as

$$dS = \frac{d\theta}{2} (r_b + r_t) \sqrt{h_s^2 + (r_b - r_t)^2}. \qquad (3)$$

The notation is illustrated in figure 3.
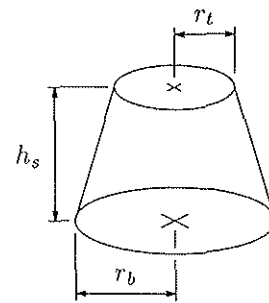
Figure 3: Notation for a Conical Frustrum Cone

The height h_s will be the difference in x-values of the two bounding helices. Since the pitch of each of the individual bounding helices in the far wake will remain constant, this height will be a linear function of the azimuth angle. That is,

$$h_s = dx = m_\theta \theta + c_\theta. \qquad (4)$$

14.4

The gradient term in the integral can be rewritten using

$$\nabla \left(\frac{1}{q} \right) = \frac{-\mathbf{q}}{q^3}. \qquad (5)$$

The derivation from here onwards progresses in a similar manner to that of Wood and Meyer [27] for their velocity influence of a semi-infinite vortex. The aforementioned assumptions are only applied were necessary for the formulation to proceed. After much algebraic manipulation, the final expression for the velocity potential is given as

$$\phi = \frac{\mu r_{v_m} N}{4\pi} \left[\frac{m_\theta r_{v_m} - p_m dr}{p_m^2} \left(\frac{1}{D_m} \right. \right.$$
$$\left. + \frac{(x_i - x_{v_m})}{(r_i^2 + r_{v_m}^2)} \left(1 - \frac{X_m}{D_m} \right) \right)$$
$$+ \frac{c_\theta r_{v_m} + (x_i - x_{v_m}) dr}{p_m (r_i^2 + r_{v_m}^2)} \left. \left(1 - \frac{X_m}{D_m} \right) \right]. \qquad (6)$$

The subscript m refers to values midway along the strip at $\theta = 0$, the start of the semi-infinite helical strip. The x axis is coincident with the axis of rotation. For a constant pitch flat helical doublet strip, this expression performs as well as that derived by Gould [11] specifically for this kind of doublet strip. The convergence of the velocity potential induced by a flat helical strip is presented in figure 4.
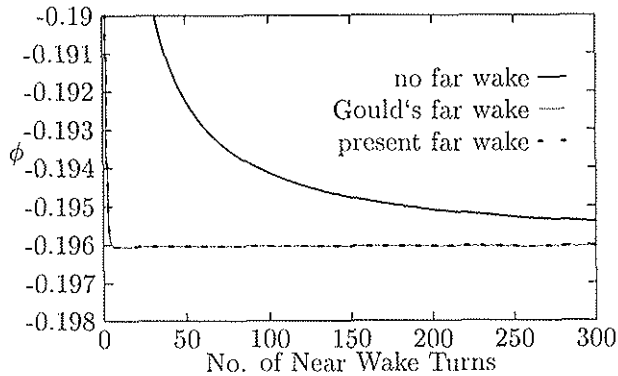
Figure 4: Convergence of the Potential for a Flat Helical, Constant Pitch Doublet Strip

The test case presented involved two flat helices of pitch $p = 0.1$, bounded by vortices at radii $r = 0.7$ and $r = 0.8$. The helices started at the positive and negative y-axis, and therefore corresponds to a two-bladed test case. The point at which the potential was evaluated was located at the Cartesian coordinate $(-0.1, 0.85, 0.0)$. A hundred segments per turn were used for the evaluation of the near wake. Figure 4 demonstrates that both the current expression and that derived by Gould, perform very well indeed for this test case.

Now test cases will be investigated for which Gould's expression is invalid (and found to be ineffective). With the previous test case both c_θ and m_θ were zero. The next two tests make each of these terms nonzero in turn, thus individually validating the terms which each accompanies. The first test is for the c_θ term. This will be identical to the previous test except that the start of the outer vortex has been moved downstream by an axial distance of 0.5. The result is shown in figure 5.
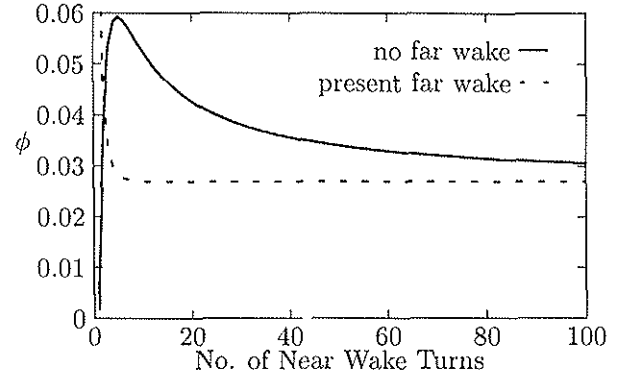
Figure 5: Convergence of the Potential for a Non-Flat, Constant Pitch Doublet Strip

To test the m_θ term, the initial test was repeated but with the pitch of the outer helix will be doubled to 0.2. The result is shown in figure 6.
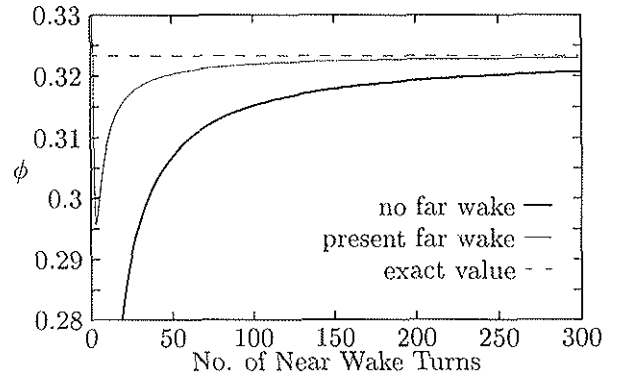
Figure 6: Convergence of the Potential for a Variable Pitch Doublet Strip

This figure demonstrates cause for concern. Note in particular the increased range of the abscissa. Whilst this is an extreme case, convergence of the expression for ϕ is very slow in comparison with the previous two cases. Despite the huge increase in efficiency that the far wake expression allows, many turns are still necessary for an accurate result.

Wake Relaxation Algorithm

The relaxation algorithm investigated is that initially devised by Butter and Hancock for fixed wings. This is best illustrated by considering a vortex filament lying within a plane. The filament is constructed from a series a straight-line vortex segments as illustrated in figure 7. The wake is relaxed a 'cross-wake' plane at a time. For each 'cross-wake' plane relaxation, the downstream planes are displaced by the same amount. This procedure is illustrated in the figure 7. This shows the steps taken during the relaxation of one wake plane of a single filament.
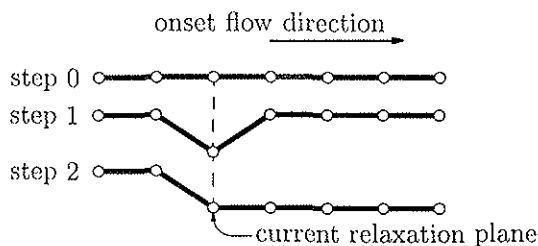
Figure 7: Schematic of Butter and Hancock Algorithm

Due to the recent success in the application to yacht sails and other high-lift wings [10], it was considered appropriate to investigate this method for rotor wake calculations.

For the case of a rotor wake, displacing the downstream nodes by the same amount applies to the radial and axial movement. The nodes are restrained to move within a plane of constant azimuth angle. Such restraint has previously been found by the current author and in other investigations [26] to aid the convergence properties. In the relaxation of each plane, the velocity at each segment across the plane is calculated. Each segment is then rotated, about its upstream node, by a given fraction (the relaxation factor) towards the local velocity vector. There still remains the issue of how to establish the velocity at a segment. In previous applications of this method, this was done by calculating the velocity at some point along the segment. Maskew [20] investigated how far along the segment this velocity should be evaluated, and concluded that the velocity should be calculated at a fractional distance of 0.55 from the upstream node. This recommendation was subsequently utilised by Gaydon [10]. For rotor wake calculations, however, a far more robust wake calculation can be achieved by averaging the velocity induced at the two ends of the segment. This enabled convergence for conditions where Maskew's recommendation failed. Whilst this increases the computation time for a given relaxation, the number of relaxations required is reduced. This aspect will be illustrated in a later section, during a comparison with the speed of other relaxation algorithms in use.

The convergence of this method discussed above was only possible for hover conditions after making a single modification to the general relaxation scheme, in addition to the automated selective merging of discrete vortices. Namely, no similar *axial* displacment of downstream vortices (step 3 in figure 7) was undertaken if the displacement was towards the rotor plane. Although this modification slows down the convergence process, it does not invalidate the process, since step 2 in figure 7 is still performed. Further, the effect of slowing down the convergence is limited by choosing an initial wake of pitch less than that of the solution. Without this modification, the root vortex (whether merged with adjacent vortices or not) tended to move above the following rotor blade, causing havoc with the blade model solution process.

After each 'cross-wake' plane relaxation, a test is made to see if any of the vortices across the current plane needed to be merged together. The exception to this is the final cross-wake plane for reasons discussed in the previous section.

Performance of the Relaxation Scheme

In order to assess the speed of the model, it was compared with a recently developed method which demonstrated quick and robust convergence. This is the method of Crouse, Bagai and Leishman [2, 8, 18]. It appears that their relaxation process has only been applied to a wake consisting of a single rolled-up tip vortex, therefore avoiding the main causes of convergence problems from the outset; namely, vortices orbiting one another and root vortices moving above the following rotor. Indeed the present author was unable to obtain convergence in hover with a full wake with only the outer two vortices merged together at the root and tip. A test case where the merging of vortices is not required for convergence was therefore found. This was achieved by only using four horseshoe vortices and a tip speed ratio of 20. For a fair comparison with the present method, the same routines for the calculation of the wake influence were used. Only the relaxation algorithm differed. A basic Euler method was also included in the comparison. The following figure shows a plot of the how the wake converges with time when using various wake relaxation algorithms. Since all the algorithms were performed for a hundred relaxations,

the extension of each line along the time axis is an indication of the time per relaxation step.

The two results for the current method (based on that of Butter and Hancock) represent the two different possiblities in establishing the velocity at a straight line segment. It can be seen that the method of averaging the velocity calculated at the two end nodes is just as efficient in terms of rate of convergence, as the method of just evaluating the velocity at a single location along the segment. This graph does indeed show the advantages of the predictor-corrector formulation. However, the present method is required for the solution of a full-wake hovering rotor prediction. As previously presented, the predictor-corrector method does not appear to be able to deliver this kind of solution, although, this could be due to the limited experience of the author with this method. Also the predictor-corrector scheme was developed for the more general case of periodic onset flows with respect to the rotor blades. As a check, it was found that both the predictor-corrector and the current method gave the same wake trajectory once they had converged.
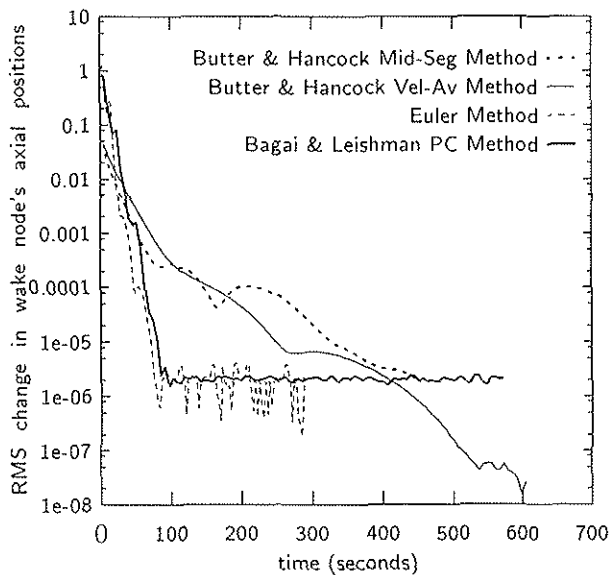
Figure 8: Comparison of Wake Algorithm Convergence Properties

Blade Models

Three models of the blade will be considered here; two lifting-line models and a surface panel method model.

The panel method is an adaption of the NEWPAN panel method program. This is a low-order potential based panel method. A constant pressure Kutta condition is applied to the trailing edge, in a similar manner to Hoshino [13].

The two lifting-line models are both non-linear, with table lookups for the aerodynamic section properties. They both require discretization of the circulation across the blade and the lifting line being located at the quarter chord line. A cosine distribution of both the trailing vortices and the collocation points is used across the blade. They only differ in the location at which the *wake-induced* velocity is evaluated. In the first method, the wake-induced velocity is evaluated at the bound vortex (the quarter chord line) as in Prandtl's classical lifting line theory [1]. In the second method, it is evaluated at the three-quarter chord line. The movement of the wake-induced velocity point to the three-quarter chord location is the result of the work of Johnson [14, 15], in trying to obtain a 'higher-order' lifting-line theory that still allowed the use of nonlinear tables for the aerofoil section characteristics. This second method will be referred to as the 'modified NLL method' from here on, and was found to produce spanwise loading predictions on a par with lifting surface theory for low aspect ratio and swept wings. In the present implementation, the wake segments are relaxed from the lifting line for the evaluation of wake induced velocities at the quarter chord. For the modified NLL method, the first row of wake segments are constrained to the chord upto the trailing edge. The wake in the modified NLL method is therefore only relaxed beyond the trailing edge location.

Comparisons with Experiment

The results of two test cases will be presented, representing different applications of the rotor, and consequently different wake characteristics. Under hovering conditions, the results of Caradonna and Tung [6] will be used. For a wind turbine example, the results obtained [9, 25] from a Stork 5WPX rotor will used for comparison.

Caradonna and Tung's Hovering Rotor

This test case [6] is often used as part of a validation procedure for numerical rotor wake methods, for several reasons. First of all, hover represents one of the most difficult flight regimes for rotor wake prediction methods. Secondly, the model is a simple, constant chord, untwisted, two-bladed rotor. The aerofoil section used was a NACA0012 section, for which two-

dimensional aerofoil data is readily available. Data was obtained for both the loading of the blade and the trajectory of the tip vortex.

Neither the root cut-out or the chord was specified in their work. A root cut-out of $0.188m$ and a chord of $0.1905m$ are used here. The radius of the model rotor was $1.143m$.

The main pitch setting of interest and commonly used for comparison was that of eight degrees. For each of the blade models, sixteen horseshoe vortices were trailed from the blade. For the relaxed and intermediate regions of the wake, each vortex filament was represented by 24 line vortex elements per turn. The fully relaxed region was extended for 80 wake segments ($3\frac{1}{3}$ revolutions). The development of the wake for the modified NLL method is illustrated in figure 9. As a demonstration of the robustness and generalisation of the wake method, the starting wake was selected as one with fixed helical pitch of 0.05.
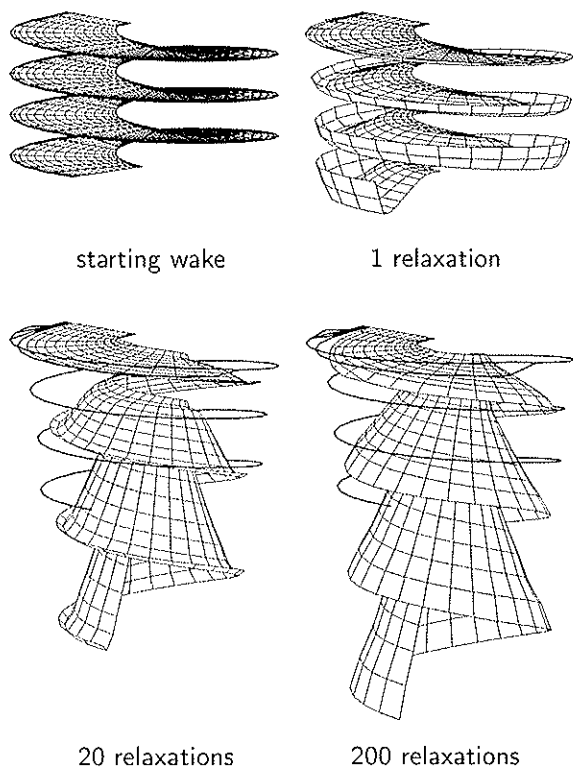
Figure 9: Development of a Hovering Rotor Wake

The distributions of thrust coefficient across the rotor for all three blade models and the experiment are given in figure 10.

The lifting line model with the wake induced velocities calculated at the quarter chord significantly overpredicts the loading near the tip. Both of the other two models compare quite well with experiment.
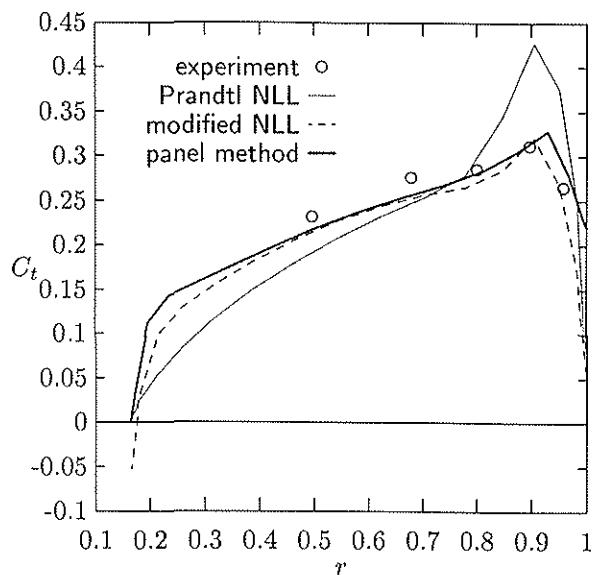
Figure 10: Load Distribution for Caradonna and Tung Rotor at 8°.
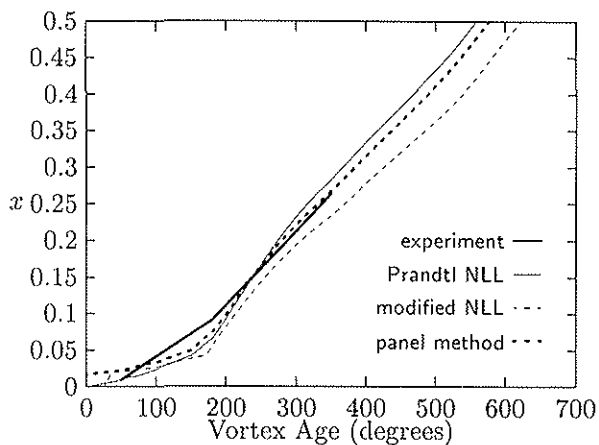
Figure 11: Axial Movement of Tip Vortex for Caradonna and Tung Rotor at 8°.
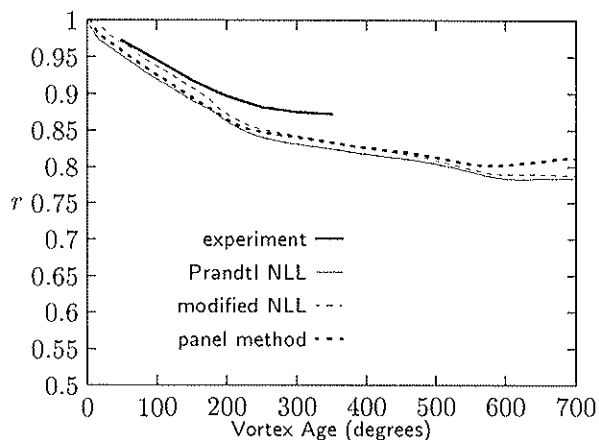
Figure 12: Radial Movement of Tip Vortex for Caradonna and Tung Rotor at 8°.

The tip vortex trajectory is illustrated in figures 11 and 12. All of the models over-predict the contraction of the tip vortex. The rate of axial movement is well predicted beyond the first blade passage. All methods, however, under predict the rate of axial movement before the first blade passage. A view of the entire converged wake obtained from the panel method application is presented in figure 13.
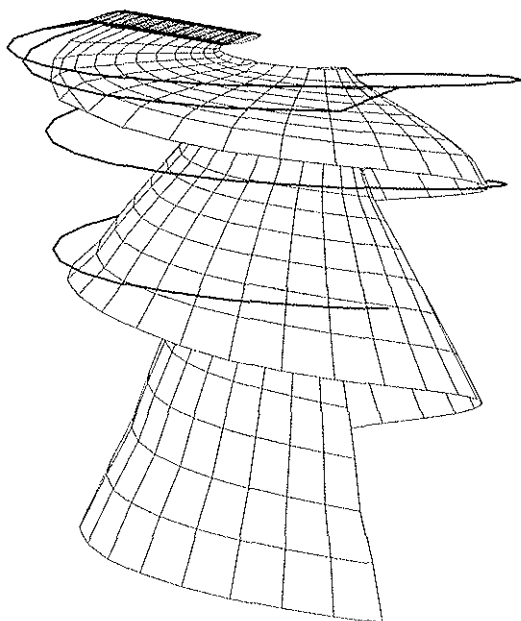
Figure 13: Converged Wake Geometry for Caradonna and Tung Rotor at 8°.

Results for the loading of the test blade at twelve degrees of pitch are presented in figure 14. Once again the loading is seen to be fairly well predicted. Comparisons of the tip vortex trajectory are illustrated in figures 15 and 16. Once again, the contraction of the wake can be seen to be over-predicted. Finally, results were obtained by Caradonna and Tung [6] for the blade pitched at five degrees. Fully converged results were unable to be obtained with the present method for any of the blade models. The cause was the upward migration of the root vortex (whether merged or not) towards the rotor plane and beyond. In the case of the lifting line models, the root vortex went above the following rotor causing non-convergence of the blade solution procedure. In the case of the panel method, the root vortex was physically unable to go above the blade, since its presence for close approach is more accurately modelled. However, due to the proximity of the root vortex to the blade, the loading of the blade towards the root was high. The solution as a whole would not satisfactorally converge. Several conclusions can be made from this final result.
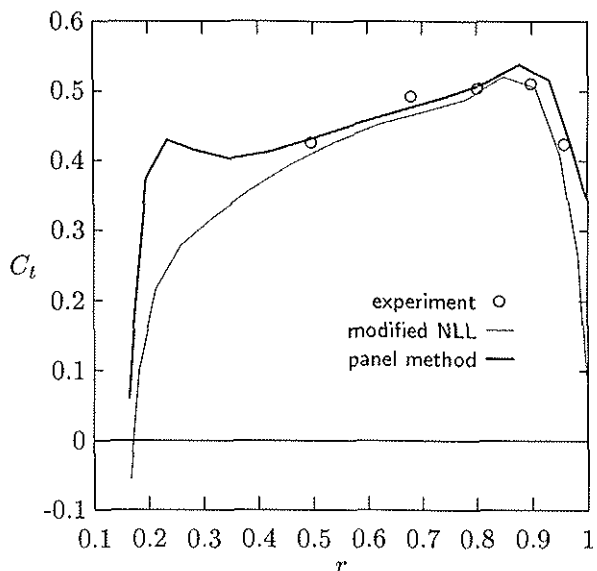
Figure 14: Load Distribution for Caradonna and Tung Rotor at 12°.
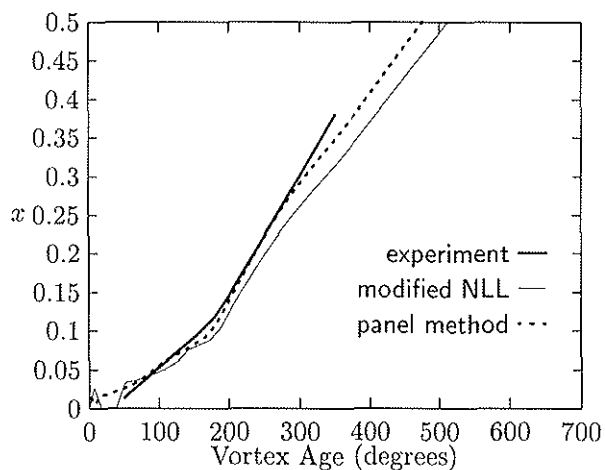
Figure 15: Axial Movement of Tip Vortex for Caradonna and Tung Rotor at 12°.
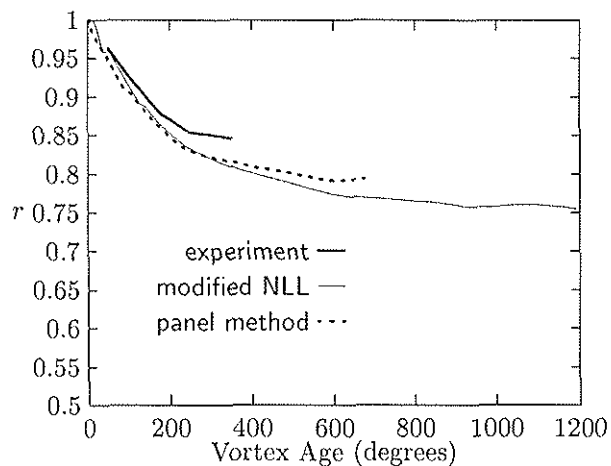
Figure 16: Radial Movement of Tip Vortex for Caradonna and Tung Rotor at 12°.

First of all, since the five degree pitch case was the lowest loaded rotor, it could be possible that the root vortex does indeed spiral upwards instead of downwards. This possibility was not accomodated within the present implementation. Finally, no vortex cores were introduced in the present model. This was to see the accuracy of performance predictions that could be obtained without the use of such empirical input. The introduction of such a core to the root vortex will reduce the velocities it induces towards the root of the blade and consequently the strength of the root vortex will also be reduced. This may prevent the movement of the root vortex above the rotor plane. However, such behaviour of the root vortex has been observed in other numerical work [19].

Stork 5WPX Wind Turbine

The test case is a two-bladed horizontal axis wind turbine[9, 25]. The quarter chord line was straight and intersected the axis of rotation. The angle of twist varies from 8° at the root to zero at the tip. The basic dimensions of the blade are presented in figure 17.
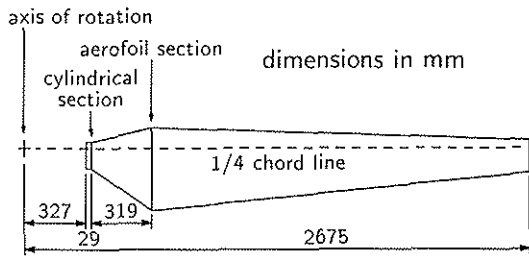
Figure 17: Basic Dimensions of the Stork 5.0 WPX Blade

The aerofoil sections used belong to the NACA 44XX series, but with the thickness aft of the maximum thickness increased slightly to make the blade more damage tolerant. NACA 44XX sections were used for the panelling of the blade. The operating condition for which attached experimental pressure distributions were available was at a tip speed ratio of 8.27. Results were obtained using a rigid wake (each wake filament being convected with the freestream velocity) and a relaxed wake calculation. The relaxed wake is shown in figure 18. For clarity only the wake from one of the two blades is shown. This was obtained by relaxing the wake for thirty iterations and solving for the body doublet strengths. The doublet strengths were thereafter solved after every ten relaxations of the wake. A total of fifty wake relaxations were performed before the doublet strengths appeared to no longer alter significantly.
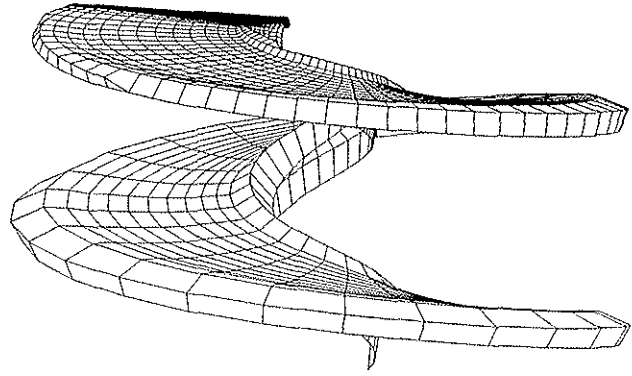
Figure 18: Converged Wake Geometry from One Stork Blade

Comparisons of the pressure distributions are shown in figures 19, 20 and 21 for the 0.3R, 0.55R and 0.75R spanwise stations respectively.
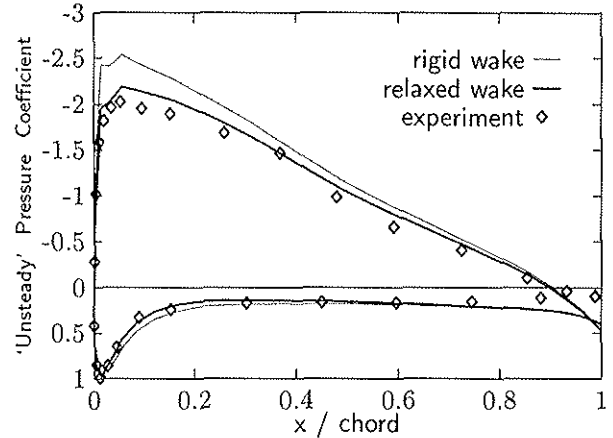
Figure 19: Distribution of Pressure Around 30% Station
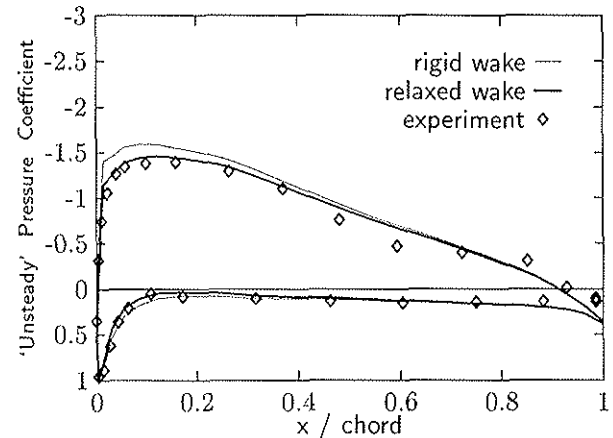
Figure 20: Distribution of Pressure Around 55% Station
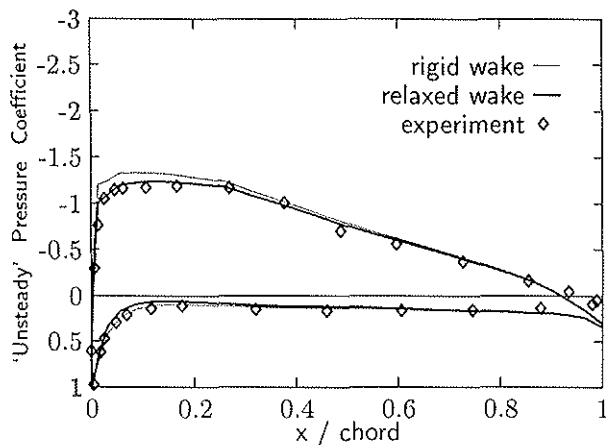
Figure 21: Distribution of Pressure Around 75% Station

It can be seen that the effect of relaxing the wake is to significantly reduce the gap between theory and experiment. The most notable difference between theory and experiment is towards the trailing edge. This difference is attributable to the theory being inviscid. The numerical coupling of a boundary layer over the aerodynamic surface and wake will reduce the increase in pressure towards the trailing edge, and thus bring the theory yet closer to the experiment.

Conclusions

Several new developments in wake methodology have been described, and their effectiveness demonstrated. The wake relaxation algorithm, new to rotor wake prediction, combined with a dynamic approach to the merging of vortices, provide a very general technique for dealing with a full span wake from any axial flow rotor configuration. Advances in the efficient calculation of the far wake have also been described. A new formulation for the accurate calculation of the velocity potential due to a far wake constructed by a series of differing pitch vortex filaments is presented. This was shown to give large reductions in the number of turns of intermediate wake required in order for the potential to be accurate to within any given accuracy. The combination of these developments were shown to give accurate predictions of the loading over a hovering rotor and wind turbine test case. However, some discrepancies were apparent between the tip vortex trajectory predicted by the method and empirical observations. In particular, the contraction of the tip vortex was consistently over-predicted. Finally, three

blade models were compared for a hovering rotor case. The panel method was shown to perform very well. A modified nonlinear lifting line theory also gave very good results for the blade loading. However, a non-linear lifting line theory based on Prandtl's lifting line method, was shown to significantly over-predict the loading towards the blade tip.

Acknowledgements

References

[1] Anderson J.D.Jr.: "Fundamentals of Aerodynamics." 2nd edition, McGraw-Hill, Inc., 1991.

[2] Bagai A.; Leishman J.G.: "Rotor Free-Wake Modeling Using a Pseudoimplicit Relaxation Algorithm." Journal of Aircraft, Vol.32, No.6, pp.1276–1285, 1995.

[3] Bliss D.B.; Miller W.O.: "Efficient Free Wake Calculations Using Analytical/Numerical Matching." Journal of the American Helicopter Society, Vol.38, No.2, 1993.

[4] Bliss D.B.; Teske M.E.; Quackenbush T.R.: "A New Methodology for Free Wake Analysis Using Curved Vortex Elements.", NASA CR 3958, December 1987.

[5] Brown K.D.; Fiddes S.P.: "Numerical Analysis of a Rigid Helical Wake Model," Report No.700, Department of Aerospace Engineering, University of Bristol, England, July 1994.

[6] Caradonna F.X.; Tung C.: "Experimental and Analytical Studies of a Model Helicopter Rotor in Hover.", Vertica, Vol.5, pp.149-161, 1981. Or NASA TM 81232, 1981.

[7] Clark D.R.; Leiper A.C.: "The Free Wake Analysis. A Method for the Prediction of Helicopter Rotor Hovering Performance.", JAHS, 15:1, January 1970. Or 25th Annual Forum of the American Helicopter Society, Preprint No. 321, May 1969.

[8] Crouse G. L.; Leishman J. G.: "A New Method for Improved Rotor Free-Wake Convergence.", AIAA paper 93-0872, 31st Aerospace Sciences Meeting & Exhibit, Reno, NV, January 1993.

[9] Dexin H.; Ming C.; Dahlberg J-Å.; Ronsten G.: "Flow Visualisation on a Rotating Wind Turbine Blade." FFA TN 1993-28, 1993.

[10] Gaydon J.H.: "Improved Panel Methods for the Calculation of Low-Speed Flow Around High-Lift Configurations." Ph.D. Thesis, Department of Aerospace Engineering, University of Bristol, England, September 1995.

[11] Gould J.: "Computational Performance Prediction Methods for Horizontal Axis Wind Turbines.", Ph.D. Thesis, Department of Aerospace Engineering, University of Bristol, England, May 1993.

[12] Hopfinger E.J.; van Heijst G.J.F.: "Vortices in Rotating Fluid Mechanics.", Annual Review of Fluid Mechanics, Vol.25, pp.241–289, 1993.

[13] Hoshino T.: "Hydrodynamic Analysis of Propellers in Steady Flow Using a Surface Panel Method." Journal of the Society of Naval Architects of Japan, Vol.165, pp.55–70, June 1989.

[14] Johnson W.: "Assessment of Aerodynamic and Dynamic Models in a Comprehensive Analysis for Rotorcraft.", Computers and Mathematics with Applications, Vol.12A, Jan. 1986.

[15] Johnson W.: "Recent Developments in Rotary-Wing Aerodynamic Theory." AIAA Journal, Vol.24, No.8, pp.1219–1244, 1986.

[16] Kim J.; Komerath N.; Liou S-G.: "Vorticity Concentration at the Edge of the Inboard Sheet." 49th Annual Forum of the American Helicopter Society, pp.585–595, 1993.

[17] Landgrebe A.J.: "An Analytical and Experimental Investigation of Helicopter Rotor Hover Performance and Wake Geometry Characteristics.", USAAMRDL TR 71-24, June 1971.

[18] Leishman J. G.; Bagai A.: "Free-Wake Analysis of Twin-Rotor Systems.", paper No. 28, 20th European Rotorcraft Forum, Amsterdam, Netherlands, October 1994.

[19] Miller R.H.: "Rotor Hovering Performance Prediction Using the Method of Fast Free Wake Analysis.", Journal of Aircraft, Vol.20, pp.257-261, 1983.

[20] Maskew B.: "A Quadrilateral Vortex Method Applied to Configurations with High Circulation.", NASA SP-405, 1976.

[21] Moore D.W.: "A Numerical Study of the Roll-Up of a Finite Vortex Sheet." Journal of Fluid Mechanics, Vol.63, Part 2, pp.225-235, 1974.

[22] Morino L.; Kuo C.C.: "Subsonic Potential Aerodynamics for Complex Configurations: A General Theory.", AIAA Journal, Vol.12, pp.191–197, 1974.

[23] Newman J.N.: "Distributions of Sources and Normal Dipoles over a Quadrilateral Panel." Journal of Engineering Mathematics, Vol.20, pp.113–126, 1986.

[24] Quackenbush T.R.; Bliss D.B.; Wachspress D.A.; Ong C.C.: "Free Wake Analysis of Hover Performance Using a New Influence Coefficient Method.", NASA CR 4309, July 1990.

[25] Ronsten G.: "Geometry and Installation in Wind Tunnels of a 5.0 WPX Wind Turbine Blade Equipped with Pressure Taps." FFAP-A 1006.

[26] Summa J.M.: "Advanced Rotor Analysis Methods for the Aerodynamics of Vortex-Blade Interactions in Hover.", Vertica, Vol. 9 No. 4, pp. 331-343, 1985.

[27] Wood, D.H., Meyer, C.: "Two Methods for Calculating the Velocities Induced by a Constant Diameter Far-Wake.", Journal of Aircraft, Vol 28, No. 8, Aug. 1991.